https://doi.org/10.5194/tc-2019-259
Preprint. Discussion started: 13 January 2020

The Cryosphere Discussions
Open Access

Terminal motions of Longbasaba Glacier and their mass contributions to proglacial lake volume during 1988–2018

Junfeng Wei[1], Shiyin Liu[2,3], Te Zhang[1], Xin Wang[1], Yong Zhang[1], Zongli Jiang[1], Kunpeng Wu[2,3], Zhen Zhang[4]

[1]School of Resource & Environment and Safety Engineering, Hunan University of Science and Technology, Xiangtan, 411201, China
[2]Institute of International Rivers and Eco-Security, Yunnan University, Kunming, 650091, China
[3]State Key Laboratory of Cryospheric Sciences, Northwest Institute of Eco-Environment and Resources, Chinese Academy of Sciences, Lanzhou, 730000, China
[4]School of Geomatics, Anhui University of Science and Technology, Huainan, 232001, China

Correspondence to: Junfeng Wei (weijunfeng@hnust.edu.cn)

Abstract. The interaction between a glacier and its glacial lake plays an increasingly important role in glacier shrinkage and proglacial lake expansion, and it increases the risk of glacial lake outburst floods (GLOFs). Longbasaba Glacier is directly contacted by a moraine-dammed lake with a high outburst risk in the central Himalayas, and has drawn a great deal of attention from scientists and local governments. Based on Landsat images and *in-situ* measurements, the evolution records of the shrinkage of Longbasaba Glacier and the corresponding expansion of its proglacial lake were determined for 1988–2018, and the mass contributions of glacier shrinkage to the increase in lake water volume were assessed. During the past three decades, Longbasaba Glacier has experienced a continuous and accelerating recession in glacier area and length but accompanied by the decelerating surface lowing and ice flow. Consequently, Longbasaba Lake has expanded significantly at an accelerating rate. The glacier surface lowering played a predominant role in the mass contribution of glacier shrinkage to the increase in lake water volume, while ice avalanches were the main potential trigger for failure of moraine dams and subsequent GLOF events. Due to the areal expansion, decreasing mass contributions from parent glacier shrinkage, and some mitigation measures by local governments to improve the drainage systems, the potential risk of outburst for Longbasaba Lake has continuously decreased during the last decade.

1 Introduction

Responding to climate warming during recent decades, the main mountain ranges across the world have exhibited continuous and accelerating glacier shrinkage (Zemp et al., 2015; Brun et al., 2017; Yang et al., 2019). The rapid reduction of mountain glaciers plays an increasingly important role in both the areal and water volume expansion of glacial lakes (Zhang et al., 2015; Song et al., 2017; Zhang et al., 2017; Yang et al., 2018), and subsequently, has increased the potential risk and destructiveness of glacial lake outburst floods (GLOFs) (Wang et al., 2016; Nie et al., 2017). For lake-terminated glaciers with debris-covered tongue, the mass/energy interactions of the thermal regime and ice avalanches between the glacier front and the lake water result in rapid glacier wastage, which creates subsequent proglacial lake expansion and is prone to causing an accelerated reduction of the parent glaciers (Carrivick and Tweed,

https://doi.org/10.5194/tc-2019-259
Preprint. Discussion started: 13 January 2020

2013; Fujita and Sakai, 2014). Eventually, lake-terminated glaciers exhibit more significant shrinkage, which provides a significant mass budget and increases the risk of GLOFs (Emmer, 2017; Zhang et al., 2019). GLOFs and their accompanying debris flows have become the predominant glacial hazard and cause ruinous impact on downstream ecosystems, communities, infrastructure, and economic developments (Fujita et al., 2008; Nie et al., 2018; Zhang et al., 2019). In the Third Pole, the majority of glacial lakes develop in the Himalayan range, and have experienced an overall areal expansion of ~14% from 1990 to 2015 (Zhang et al., 2015; Nie et al., 2017). In this region, potentially dangerous glacial lakes are widely distributed (Wang et al., 2012, 2015), and more than 70 GLOF events have been reported (Khanal et al., 2015; Veh et al., 2018). Approximately 80% of the reported GLOFs were initiated by an abundant ice mass suddenly entering a proglacial lake due to ice avalanches on the glacier terminal (Awal et al., 2010; Nie et al., 2018).

Longbasaba Lake is a typical potentially dangerous glacial lake with a higher outburst risk in the Himalayas (Wang et al., 2015; Wang et al., 2018). A lake outburst in this location would significantly threaten the livelihoods and activities of the local people in downstream countries, for example, the transportation/communication facilities and hydropower stations (Yao et al., 2012). Hence, the evolution of Longbasaba Glacier/Lake and their mass interactions are necessary in order to assess the prediction of GLOF events and gain the attention of scientists and local government departments (Wang et al., 2008; Yao et al., 2012; Nie et al., 2017; Wang et al., 2018). In this study, we aim to assess the mass contribution of glacier shrinkage to the increase in lake water volume by monitoring the motions of the glacier terminal and subsequently to extract the ratios of the mass budgets contributed by the ice flow/retreat of the glacier terminal and the changes in the glacier surface elevations. Finally, the retreat patterns of the parent glacier and their impacts on the proglacial lake are discussed.

2 Study area

Longbasaba Glacier is contacted by a moraine-dammed lake and located at the source area of the Pumqu River on the northern slope of the central Himalayas (Fig. 1a). This glacier covered an area of 28.4 km^2 in 2010, with a length of 8.7 km and a debris-covered area of 1.06 km^2 on the tongue (3.7%) (Guo et al., 2015). There are numerous serac clusters and small supraglacial lakes on the glacier tongue (Fig. 1b). Many crevasses have formed in the glacier front and commonly cause ice avalanches, which causes ice floe masses of various sizes over the surface of the proglacial lake (Fig. 1c). Longbasaba Lake is in direct contact with the parent glacier and remains at a high risk of outburst (Wang et al., 2016). The proglacial lake had an area of 1.22 km^2 in 2009, with a maximum length of 2.210 km from east to west and a maximum width of 0.685 km from south to north (Yao et al., 2012). According to the *in-situ* measurements taken using an echo sounder in 2009, the water level of Longbasaba Lake was 5499 m and the average and maximum depths were 48 m and 102 m, respectively, with a water volume of 0.064 km^3 in 2009 (Yao et al., 2012). The glacier front retreated by 1264 m (40 m a^{-1}) from 1977 to 2009, which resulted in a glacial lake expansion of 223%. In addition, an accelerating recession of the glacier terminal (63.8 m a^{-1}) was observed from 2005 to 2009, with a rapid areal expansion rate of 0.040 km^2 a^{-1} for Longbasaba Lake (Wang et al., 2016).

https://doi.org/10.5194/tc-2019-259
Preprint. Discussion started: 13 January 2020

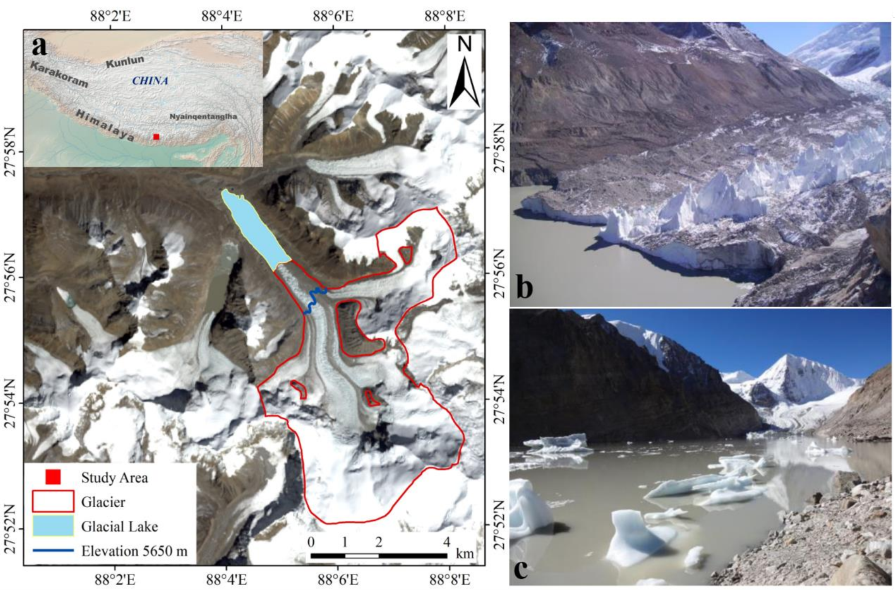

Figure 1. (a) The study area. The outlines of Longbasaba Glacier/Lake were detected from the Landsat OLI image taken in 17 October 2018. The background of the eagle-eye map was available from Natural Earth. The blue line shows the location of the ice fall. **(b)** Crevasses, serac clusters and debris cover occurred over the glacier tongue. Some ice avalanches could be found at the flank of the glacier terminal. **(c)** Ice floes widely distributed over the lake surface.

3 Data and methods

3.1 Glacier reduction and lake expansion

The outlines of Longbasaba Glacier/Lake during the 1988–2018 period were manually generated from Landsat TM\ETM+\OLI images using pan-sharpening employing principle-component analysis. These multispectral, multitemporal images are available for free from the United States Geological Survey (USGS). They are orthorectified with the SRTM DEM and ground-control points from the Global Land Survey 2005 (GLS2005), with a spatial resolution of 30 m and a WGS1984/EGM1996 coordination system (Woodcock et al., 2008). The horizontal accuracies of the Landsat images are better than one pixel to each other or to non-differential GPS data (Bolch et al., 2010; Guo et al., 2015).

In total, 34 Landsat TM\ETM+\OLI images acquired during the investigation period were used in this study (Tab. 1). The Landsat images covering the region of interest were dramatically affected by frequent snow and cloud cover. Then, we preferentially choose the Landsat images acquired in September and October without snow and cloud cover. Other high-quality images acquired in the adjacent months (e.g., July and August) were used to detect the precise outlines of the glacier and lake when there was no perfect image from September or October. In addition, scanline errors (SLC-off scenes acquired by the ETM+ sensor since early summer 2003) also created obstacles in generating the glacier/lake outlines. Then the SLC-off images were used only to define the positions of the glacier front.

https://doi.org/10.5194/tc-2019-259
Preprint. Discussion started: 13 January 2020

Table 1. Landsat images utilized to detect the terminal retreat and ice flow of Longbasaba Glacier. Images* with heavy cloud cover or scanline errors (SLC-off scenes) were just for the position generation of the glacier front.

Date	Image ID	Sensor	Date	Image ID	Sensor
1988/09/12	LT51390411988256BKT00	TM	2003/11/25	LT51390412003329BKT00	TM
1989/09/23	LT41390411989266XXX01	TM	2004/10/10	LT51390412004284BKT00	TM
1990/06/14	LT51390411990165BKT00	TM	2005/10/13	LT51390412005286BKT00	TM
1991/09/21	LT51390411991264BKT00	TM	2006/10/16	LT51390412006289BKT00	TM
1992/09/23	LT51390411992267BKT00	TM	2007/10/03	LT51390412007276BKT01	TM
1993/10/12	LT51390411993285BKT00	TM	2008/10/21	LT51390412008295BKT00	TM
1994/09/29	LT51390411994272ISP00	TM	2009/09/22	LT51390412009265KHC00	TM
1995/04/09	LT51390411995099BKT01	TM	2010/06/21	LT51390412010172KHC00	TM
1996/10/20	LT51390411996294ISP00	TM	2011/06/08	LT51390412011159BKT00	TM
1997/07/03	LT51390411997184BKT01	TM	2013/12/22	LC81390412013356LGN01	OLI
1998/10/10	LT51390411998283BKT00	TM	2014/10/06	LC81390412014279LGN01	OLI
1999/05/22	LT51390411999142BKT00	TM	2015/10/09	LC81390412015282LGN01	OLI
2000/10/15	LT51390412000289BKT01	ETM+	2016/10/11	LC81390412016285LGN01	OLI
2001/10/26	LE71390412001299SGS00	ETM+	2017/10/30	LC81390412017303LGN00	OLI
2002/10/29	LE71390412002302SGS00	ETM+	2018/10/17	LC81390412018290LGN00	OLI
1995/07/30	LT51390411995211BKT00*	TM	2012/10/08	LE71390412012282PFS00*	ETM+
2010/10/03	LE71390412010276SGS00*	ETM+	2013/10/11	LE71390412013284SG100*	ETM+

Subsequently, the areal variations in Longbasaba Glacier/Lake during the investigation period were generated, and the main flowlines were extracted to assess the changes in the glacier length. By combining the variations in the position and shape of the glacier front during specific periods, the patterns of the terminal motions were assessed, including terminal retreat and ice avalanches. The changes in the surface elevation of Longbasaba Glacier were extracted from the High Mountain Asia Gridded Glacier Thickness Changes from Multi-sensor DEMs, Version 1 (HMA_Glacier_dH) during two subsequent time periods of 1975–2000 and 2000–2016 (Maurer et al., 2018). This data was extract based on a series of stereo scenes from KH-9 HEXAGON in 1975 and ASTER data acquired from 2000 to 2016 by fitting robust linear trends. The data used is available for free from National Snow and Ice Data Center (NSIDC), with a horizontal resolution of 30 m. The asserted accuracy of the full data is ± 0.42 m a^{-1} as derived from the non-glacier terrain (Maurer et al., 2018). Nevertheless, we obtained a higher accuracy of ± 0.04 m a^{-1} for the two investigation periods using the method of Burn et al. (2017).

3.2 Characteristics of glacier surface velocity

The Landsat images described above were also used to extract the glacier surface velocity field from image pairs based on cross-correlation feature tracking processing using the free software module Co-registration of Optically Sensed Images and Correlation (COSI-Corr) (Leprince et al., 2007; Gantayat et al., 2014; Ruiz et al., 2015; Ayoub et al., 2017). A co-registered image pair containing two Landsat images was iteratively cross-correlated on sliding windows. Finally, two horizontal ground offset fields

(East\West and North\South) and a signal-to-noise ratio (SNR) were calculated for each pixel. The SNR value reflects the quality of the registration. The surface velocity of an individual pixel was subsequently generated by combining two horizontal offsets with a higher SNR threshold of >0.95.

The mean surface velocity of the glacier (MSVG) was extracted over the glacier terrain with a maximum displacement threshold of 50 cm d^{-1}. In addition, the mean surface velocity of the glacier tongue (MSVT) was generated by averaging the velocities with the same threshold of pixels over the glacier tongue region with an altitude of less than 5650 m where ice fall occurred for Longbasaba Glacier. Unfortunately, there was no perfect Landsat pair to extract the glacier surface velocity for 2012, so the surface velocity from 2011–2013 was calculated instead using the individual velocity maps for 2011–2012 and 2012–2013. Finally, the extra-annual characteristics of the MSVG and MSVT were detected and discussed.

The monthly mean velocities indicate that the intra-annual variations in ice flow and were analyzed from the GoLIVE (Global Land Ice Velocity Extraction from Landsat 8, Version 1) data set with a time difference of 16 days during 2013–2019. The GoLIVE data set contains the glacier surface velocities with a spatial resolution of 300 m and is available for free from the National Snow and Ice Data Center (NSIDC) (Scambos et al., 2019). This data set was extracted using COSI-Corr and Landsat 8 panchromatic images obtained from 2013 to present (Fahnestock et al., 2015), and provides the glacier surface velocities with a time interval of multiples of 16, for example, 16, 32, 48, and 64 days, with accuracies ranging between ~1 m d^{-1} to 0.02 m d^{-1}. In this study, we used a total of 55 ice velocity tiles during the period of 2013-10-20 to 2019-1-6 to analyze the intra-annual characteristic of the surface velocities of Longbasaba Glacier. However, the surface velocity values from June to September were not enough to exhibit the ice flow pattern. Then, a quadratic polynomial fitting was performed to assess the ice flow during specific months, and the horizontal movements of the glacier during different seasons were determined.

3.3 Basin morphology and water volume of the glacial lake

In-situ measurements of the water depths of Longbasaba Lake were taken in September 2009 using a comprehensive measuring system containing an echo sounder and a GPS receiver (Yao et al., 2012). A total of 39, 558 echo sounder points with positions were collected. In addition, another 33 random points were obtained using a measuring rope to evaluate the accuracy, which indicated an error of less than 2 m for the water depth measurements.

Combining the water depth measurements and the lake boundary in 2009, the depth of each pixel within the lake basin was obtained using the ordinary Kriging interpolation Method. In the Himalayas, the majority of lake expansions occur with ignorable fluctuations of lake water level (Song et al., 2017; Zhang et al., 2017), and thus, we assume that the water level of Longbasaba Lake remained stable during the investigation period at the constant water level of 5499 m, which was measured by Yao et al. (2012). Subsequently, the basin morphology of Longbasaba Lake in 2009 was reconstructed.

Since Longbasaba Glacier is a typical, huge valley glacier with a flat tongue, we assume that the hypsography of the lake basin could approximately indicate the topography of the glacier bed close to

https://doi.org/10.5194/tc-2019-259
Preprint. Discussion started: 13 January 2020

the terminal. Previous studies have revealed that large glacial lakes only form in areas where the glacier surface gradient is less than 2º (Reynolds, 2000; Quincey et al., 2007). Thus, in this study, the contour lines of the lake basin (interval of 20 m) were extracted and were subsequently extrapolated to the lake basin with the maximum area in 2018 and a gradient of 2º. Finally, the basin morphology of the proglacial lake in 2018, which has a spatial resolution of 30 m, was reconstructed based on these contour lines, water depth measurements, and the lake boundary. Based on the basin morphology and lake boundaries for the different years, the lake water volumes in each year, V_l, were estimated using the following equation:

$$V_l = \sum_{i=1}^{N_l} h_l^i \, s, \tag{1}$$

where N_l is the pixel number within the lake polygon in each year, h_i^l is the depth of the individual pixel, and s is the area of an individual pixel with a value of 900 m^2.

3.4 Mass contributions of glacier wastage to lake water volume

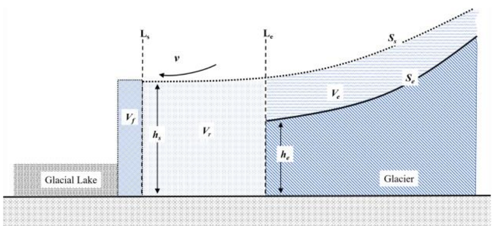

Figure 2. Mass budgets contributed by the glacier wastage to the lake water volume. L_s is the glacier front in the first year, and L_e is the glacier front after retreat in the second year. V_e is the glacier volume loss contributed by the glacier surface lowing, V_f and V_r are the ice losses contributed by the ice flow and terminal retreat, respectively.

Due to the effects of climate warming and the formation of proglacial lakes, the mass wastage of lake-terminated glaciers predominantly results from ice melt and avalanches and is characterized by terminal retreat and surface lowering (Fig. 2). Consequently, the impacts of glacier change on lake water volume can be divided into two portions: mass contribution from terminal motions, M_t, and mass contribution that is not from terminal motions, M_{nt}. The former can be further divided into two phases: terminal advance due to the ice flow of the glacier tongue and synchronous terminal retreat due to ice melt and avalanches from the glacier front. Eventually, the impact of the glacier wastage on the lake water volume can be classified into three synchronous components of mass budgets contributed by: (i) ice flow, V_f; (ii) terminal retreat, V_r; and (iii) changes in the surface elevation over the area higher than L_e, V_e (Fig. 2). Then, the mass contributions of the glacier changes to the lake water volume were calculated using the following equation:

$$M_G = M_t + M_{nt} = (V_f + V_r)\rho_{ice} + V_e \rho_{gla}, \tag{2}$$

where ρ_{ice} is the density of the ice in the glacier tongue, and a constant value of 900 kg m^{-3} was used for the ice-to-mass conversation, as recommended by Kääb et al. (2012). ρ_{gla} is the average density of the glacier for a long-time scale estimation, with a value of 850 ± 60 kg m^{-3} (Huss, 2013).

https://doi.org/10.5194/tc-2019-259
Preprint. Discussion started: 13 January 2020

The ice volume contributed by the ice flow of the glacier terminal could be estimated using the following equation:

$$V_f = \frac{vt}{R}\sum_{i=1}^{N_f} h_s^i\, s, \quad (3)$$

where v is the average surface velocity of the glacier tongue; t is the interval of the investigation periods; R is the spatial resolution of the pixel; N_f is the pixel number within the profile of the glacier front; and h_s^i is the glacier thickness for an individual pixel in the previous year. The glacier bottom layer flows slower than the upper layer, with a speed of about 30-80% of the surface velocity (Perutz, 1949; Mathews, 1959; Harper et al., 2001; Copland et al., 2003). In this study, we chose 70% of the MSVT as the value of v. The thickness of the glacier terminal could be calculated by comparing the elevations of the surface and the bed of the glacier front in a specific year. The surface elevation of Longbasaba Glacier in 1980 was extracted from the 1:50,000 Chinese historical topographic map (Wei et al., 2015; Wu et al., 2018). By combining the position and bed elevation of the glacier front, the thicknesses of the glacier front from 1988 to 2018 were generated and modified using the average surface-lowering rate of the glacier tongue, which were extracted from HMA_Glacier_dH data described in *Sect. 3.1* with the values of approximately -0.89 ± 0.04 m a^{-1} during 1975–2000 and -2.04 ± 0.04 m a^{-1} during 2000–2016.

The mass volume contributed by the retreat of the glacier front was evaluated using the following equation:

$$V_r = \sum_{i=1}^{N_r} h_s^i\, s, \quad (4)$$

where N_r is the number of pixels over the terrain between the profiles of L_s and L_e. The changes in the ice volume contributed by lowering of the surface elevation, V_e, can be estimated using the following equation:

$$V_e = \overline{h_\Delta} s_g, \quad (5)$$

where s_g is the glacier area; and $\overline{h_\Delta}$ is the average lowering rate of the glacier surface higher than L_e. The mean changes in glacier surface elevation during the two periods of 1975–2000 and 2000–2016 were extracted from the HMA_Glacier_dH data set.

3.5 Accuracy analysis

The geolocation errors of the pixels on the glacier/lake boundaries generated through a careful manual approach that can be controlled with a subpixel accuracy of approximately 0.5 pixels. The accuracies of the generated area are defined by the buffer around the glacier/lake perimeters and are equal to 0.5 pixels multiplied by the pixel number within the perimeters and the spatial resolution of the images. According to pan-sharpening employing principle-component analysis, Landsat TM\ETM+\OLI images can exhibit an optimized usage with a spatial resolution to 15 m (Wu et al., 2018). Thus, the uncertainties in the generated area of the glacier and lake are ~1% and ~28%, respectively. The accuracy of the main flowline length was also controlled within 0.5 pixels (~± 8 m).

Based on the assumption that the outline of the glacier accumulation zone remained stable during the investigation period, the areal measurements were compared to assess the image-image evolution of the glacier and lake. The errors in the areal changes in the glacier and lake were relatively small for a control

https://doi.org/10.5194/tc-2019-259
Preprint. Discussion started: 13 January 2020

approach and can be evaluated using the flowing equation (Krumwiede et al., 2014; Haritashya et al., 2018):

$$e_{ac} = n * R^2/\sqrt{m}, \qquad (6)$$

where n and m are the numbers of pixels and vertices, respectively, of the digital polygon defining the change in the area during the specific period. Finally, the accuracy of the changes in the glacier and lake areas was approximately ± 0.003 km^2.

The water volume was calculated by multiplying the lake depth and area, and then, the accuracy of the estimated water volume was assessed using error propagation. The interpolated accuracy of the lake basin depth is ± 4.87 m, which was obtained by comparing the interpolated points and the *in-situ* measurements. Considering the accuracy in the lake depth was less than 2 m based on *in-situ* measurements, the final accuracy of the lake basin depth is ± 5.26 m.

According to the error propagation, the accuracies of the mass contributions from the glacier terminal motions and surface lowering were controlled by the errors in the glacier surface velocities, thicknesses, and thinning rates. The estimation accuracy of the surface velocity was determined from non-glacier and stable terrain in the investigated region, in order to eliminate the influence of bedrock movements. The uncertainty in the glacier thickness was determined by the elevations of the glacier surface and the lake basin. Both the accuracies of the topographic maps and the elevation lowering rate of the glacier tongue determined the precision of the elevations of the glacier surface. The error in the lake depth was used to assess the accuracy of the lake basin. The uncertainty in the glacier thinning rate and the elevation lowering rate of the glacier tongue, depend on the precision of the HMA_Glacier_dH data set, which is approximately equal to ± 0.04 m a^{-1} for the two periods of 1975–2000 and 2000–2016.

4 Results

4.1 Glacier retreat and lake expansion

Longbasaba Glacier has experienced continuous and accelerating areal recession during 1988–2018, with an inhomogeneous tendency toward terminal retreat in the different phases (Fig. 3). Overall, the glacier area has decreased by 0.988 ± 0.093 km^2 since 1988, and had decreased to 29.551 ± 0.308 km^2 by 2018 with a mean decrease ratio of 3.23% (0.11% a^{-1}) during the past 30 years. Due to the parent glacier degradation in area, Longbasaba Lake has expanded from 0.604 ± 0.209 km^2 in 1988 to 1.591 ± 0.389 km^2 in 2018, with an increasing ratio of 164% relative to the lake area in 1988. Before 2008, the glacier area decreased with a dramatic fluctuation (Fig. 3). The greatest area loss occurred from 1993 to 1994, causing an area of 0.089 ± 0.003 km^2 (0.29%) to disappear based on the total glacier area in 1993. During the periods of 2000–2001 and 2003–2004, this glacier also experienced the most significant recession, with areal changes of 0.078 ± 0.003 km^2 and 0.076 ± 0.003 km^2, respectively. However, the total area of Longbasaba Glacier decreased by less than 0.05 km^2 during the other periods before 2008. In particular, during the periods of 1988–1989, 1989–1990, 1991–1992, 1994–1995, and 2004–2005, this glacier remained nearly stable with an area loss of less than 0.01 km^2. Longbasaba Glacier has retreated with a relatively stable ratio during the recent decade, and the range of areal recession has varied from 0.026 ±

https://doi.org/10.5194/tc-2019-259
Preprint. Discussion started: 13 January 2020

0.003 to 0.044 ± 0.003 km^2. Overall, the glacier has experienced accelerating shrinkage with a mean areal recession rate of 0.032 ± 0.003 km^2 a^{-1}. Nevertheless, a decelerating tendency of glacier degeneration in the area occurred during the most recent decade, but with a mean area loss rate of 0.035 ± 0.003 km^2 a^{-1}, which is greater than the overall mean recession rate from 1988 to 2018.

The length of the main flowline of Longbasaba Glacier was 8274 ± 8 m in 2018, and decreased by 1577 ± 11 m (52.6 ± 0.4 m a^{-1}) from 1988 to 2018, with a mean recession ratio of 16.01% (0.53% a^{-1}) relative to its length in 1988. The decreasing trend in length is similar to that of the glacier area (Fig. 3), that is, the fluctuation in the changes during the last decade was significantly smoother than that during 1988–2008. The most dramatic length recessions occurred during the periods of 1993–1994, 2000–2001, and 2003–2004 when the glacier experienced a length retreat of >180 m a^{-1}. Nevertheless, the main flowline showed a slight change in the length within a pixel or remained nearly stable in the other periods before 2008. From 2008–2018, the differences between the length changes were less than 22 m (55 ± 11–76 ± 11 m), except for the periods of 2014–2015 (32 ± 11 m) and 2017–2018 (42 ± 11 m). Overall, the glacier experienced an increase in length recession during 1988–2018, similar to the trend in areal recession, but with a higher mean length retreat (58.1 ± 1.1 m a^{-1}) than the period of 1988–2008 (49.8 ± 0.6 m a^{-1}). However, a slight decrease in the length recession rate was observed during the last decade.

The geodetic estimation from the HMA_Glacier_dH data set reveals continuous, decelerating mass wastage for Longbasaba Glacier. Overall, the glacier surface elevation has decreased by -0.34 ± 0.04 m a^{-1} from 1975 to 2016. The lowering rate of the glacier surface was -0.38 ± 0.04 m a^{-1} from 1975 to 2000, contributing a total mass loss of 0.128 ± 0.014 km^3 from 1988 to 2000. Based on the variations in the glacier area, the thinning rate slightly decreased to -0.28 ± 0.04 m a^{-1} from 2000 to 2016, releasing an approximate mass budget of 0.138 ± 0.020 km^3 during 2000–2018. Finally, Longbasaba Glacier has exhibited an average mass balance of -0.27 ± 0.04 m w.e. a^{-1} during the investigation period. In contrast, the glacier tongue has experienced an accelerating lowering in surface elevation from 1975–2016, with higher thinning rates ranging from -0.89 ± 0.04 m a^{-1} before 2000 to -2.04 ± 0.04 m a^{-1} from 2000 to 2016.

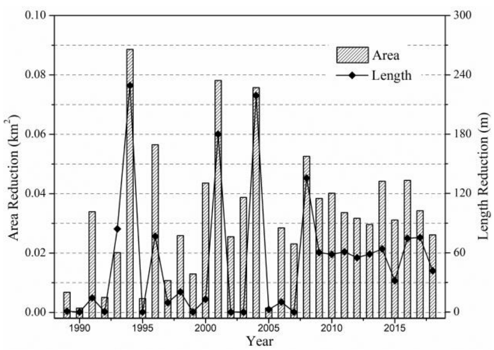

Figure 3. Comparison between changes in the area and length of Longbasaba Glacier during 1989–2018. The changes in the glacier length was detected by combining the main flowline and front potions of the glacier. The changes in the glacier area was estimated just by considering the motions of the glacier terminal.

https://doi.org/10.5194/tc-2019-259
Preprint. Discussion started: 13 January 2020

It should be noted that the flanks of the glacier terminal retreated at a different rate than the center before 2008, while the rates of the flanks and the center of the glacier were similar from 2008 to 2018 (Fig. 4). This is manifested by the fact that the amplitude and phase of the fluctuations in the changes in the glacier area and length were not completely synchronous, and this mismatch indicates the specific patterns of terminal retreat in different periods. For example, the fact that the glacier area decreased significantly while the main flowline remained nearly stable means that the center of the glacier terminal has experienced a slight retreat, while a huge area loss occurred on the flanks, which means that large-scale ice avalanches at the flanks of the terminal were the main characteristics of the terminal retreat during this period. By comparing the retreat amplitudes of the changes in the glacier area and length, the patterns of terminal retreat were divided into three categories (Fig. 5):

1) *The area and length simultaneously and significantly decreased,* for example*, in 1993–1994, 2000–2001, and 2003–2004, huge ice avalanches occurred at the center of the glacier terminal*
2) *The area retreated significantly with nearly stable length,* for example, *in 1990–1991,1999–2000, 20001–2003, and 2005–2007, huge ice avalanches occurred at the flanks of the glacier terminal*
3) *The area and length decreased with similar fluctuation,* for example*, in 2009–2018, the glacier terminal retreated as a whole due to small-scale ice avalanches*

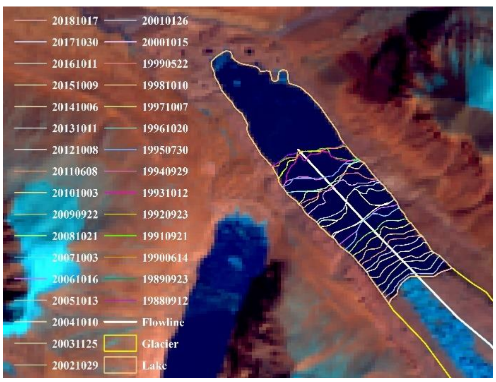

Figure 4. Variations in the front positions of Longbasaba Glacier generated from Landsat images during 1988–2018. The background map is the Landsat OLI image taken in 17 October 2018. The white line shows the main flowline of Longbasaba Glacier and exhibits the characteristic of changes in glacier length combined with the positions of the glacier front.

https://doi.org/10.5194/tc-2019-259
Preprint. Discussion started: 13 January 2020

The Cryosphere Discussions
Open Access
EGU

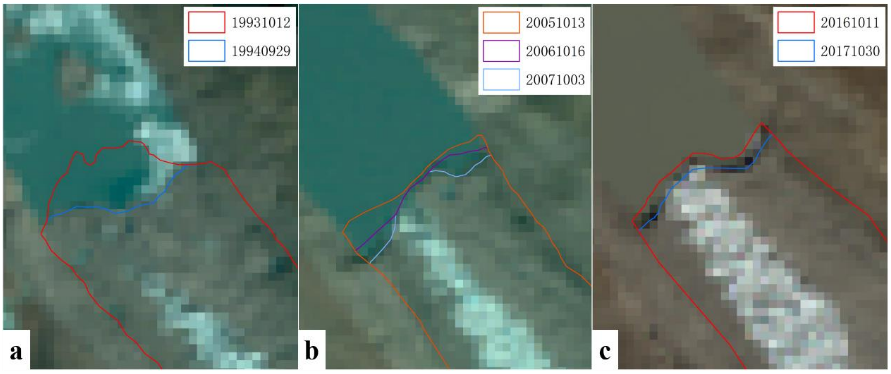

Figure 5. Three categories representing different patterns of terminal retreat of Longbasaba Glacier in specific periods. The background maps are Landsat TM\OLI images taken in 1994, 2007, and 2017, respectively. **(a)** shows the *Category 1*, with huge ice avalanches occurred at the center of the glacier terminal. **(b)** shows the *Category 2*, with huge ice avalanches occurred at the flanks of the glacier terminal. **(c)** shows the *Category 3*, with a whole terminal retreat for the glacier terminal.

These three categories of patterns of terminal retreat reveal different processes of ice masses entering the proglacial lake from the glacier terminal. *Categories 1* and *2* suddenly release numerous ice masses accompanied by debris cover into the glacial lake and potentially cause huge waves, which put pressure on the moraine dams and increase the failure risk of the moraine-dammed lake. In contrast, *category 3* releases small-scale ice avalanches with an insignificant mass budget from the glacier terminal, which would not obviously increase the risk of GLOFs for Longbasaba Lake.

4.2 Characteristics of the glacier surface velocity

The MSVG shows a decreasing trend during 1989–2018, with a similar trend for both the glacier and the glacier tongue (Fig. 6). The MSVT was 4.95 ± 1.03 cm d^{-1} during the investigation period, which is significantly greater than the MSVG (3.55 ± 1.03 cm d^{-1}), but it decreased more significantly later.

The fluctuation in the variations in the MSVT during the different periods was significant and was much greater than that of the MSVG, but both experienced synchronous fluctuations. The MSVTs were higher than the MSVGs during 1988–2018, except for 1989–1990 and 1997–1998, during which the MSVGs were slightly higher than the MSVTs. Consequently, a gentler fluctuation in the MSVG was found, according to the less significant fluctuation in the surface velocity of other zones compared to the glacier tongue. The trend in the changes in the MSVG does not agree with the changes in the glacier area and length, with correlation coefficients of less than 0.3. This reveals that the relationship between ice flow and the reductions in the glacier area and length is not clear.

https://doi.org/10.5194/tc-2019-259
Preprint. Discussion started: 13 January 2020

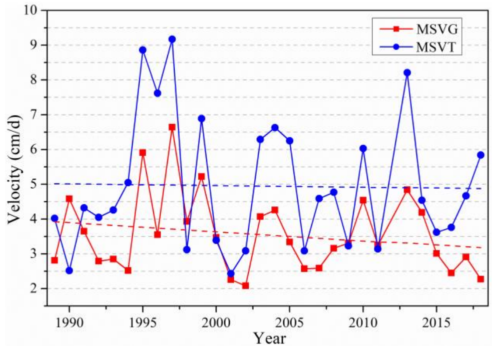

Figure 6. Mean surface velocities for the whole glacier (MSVG) and glacier tongue (MSVT) during the investigation period of 1989–2018. The blue and red dotted lines were given by the linear fitting method and show the decelerating ice flow for Longbasaba Glacier.

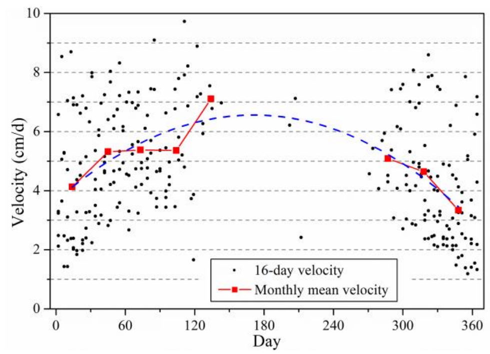

Figure 7. Intra-annual variations in the surface velocities of Longbasaba Glacier generated using GoLIVE. The black points show the mean velocities in the middle of 16 days. The values of 16-day velocities in summer and autumn were rare. The monthly mean velocities in summer and autumn were interpolated by applying the quadratic polynomial fitting method (blue dotted curve) based on the monthly mean velocities in spring and winter.

The seasonal MSVGs were calculated using GoLIVE (Fig. 7). The MSVGs were distributed predominantly in winter and spring (from October to May in the next year). Then, by applying a quadratic polynomial fitting, we assessed the MSVGs in summer and autumn (from June to September). The fastest ice flow occurred in summer (May, June, and July), and the velocity of the glacier surface decreased in spring (February, March, and April) and autumn (August, September, and October), with a flow rate of 86% and 89% of the summer velocity, respectively. The slowest glacier surface movements occurred in winter (November, December, and January in the next year) when the ice flowed at a ratio of just 62% and 73% compared to the MSVGs in the summer and the annual average velocity, respectively.

4.3 Changes in the water volume of the glacial lake

Based on the estimated basin morphology of Longbasaba Lake (Fig. 8a), the maximum depth of the glacial lake was 99.52 ± 5.26 m in 2018. A continuously increasing trend in the mean depth of the glacial

https://doi.org/10.5194/tc-2019-259
Preprint. Discussion started: 13 January 2020

lake before 2010 was accompanied by a slight decrease during the last decade, due to an elevation rise with a slight slope and the narrower width of the lake basin.

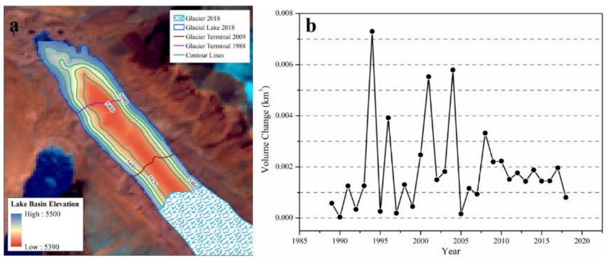

Figure 8. (a) Basin morphology of Longbasaba Lake reconstructed based on the echo sounder points in 2009 and the lake boundary in 2018. The background map is the Landsat OLI image taken in 2018. The basin morphology within the lake boundary in 2009 was generated directly from the *in-situ* measurement points and the other part was extrapolated. The deepest point (5400 m) is located at the center of the glacier terminal in 1988. **(b)** Volume changes of Longbasaba Lake estimated based on the basin morphology and changes in the lake boundary during 1988-2018.

Combing the lake depth and outlines, the water volume of the glacial lake approached a maximum value of 0.080 ± 0.022 km^3 in 2018. The water volume of the proglacial lake has increased by 233% (0.002 ± 0.001 km^3 a^{-1}) from 1988 to 2018. The most significant expansions in the lake volume occurred in the three periods of 1993–1994, 2000–2001, and 2003–2004, with expansion rates of >0.005 km^3 a^{-1}. These periods agree with the time when the glacier front retreated as described by *Category 1*. In addition, the studied lake experienced insignificant changes (< 0.0005 km^3 a^{-1}) in water volume during the periods of 1989–1990, 1991–1992, 1994–1995, 1998–1999, and 2004–2005. According to the dramatic fluctuation in the variations in the changes in the glacier area, the differences in the lake volume during different periods were significant before 2008 (Fig. 8b). However, the increasing water volume slowed slightly from 2008 to 2018.

4.4 Mass contributions of glacier shrinkage to lake water volume

The mass budget of glacier motions was predominantly contributed by the glacier surface lowering (Fig. 9). The change in the glacier surface elevation contributed more than 80% of the total mass contributions from glacier reduction including ice melt and avalanches. In particular, from 1989 to 1990, more than 90% of the mass budget resulting from glacier shrinkage was contributed by elevation changes in the glacier surface. During 1993–1994, 2000–2001, and 2003–2004, when Longbasaba Glacier retreated as described in *Category 1*, the proportions of the mass contributions from the lowering of the glacier surface decreased to approximate 50%, which suggests that the mass contributions from the glacier motion have increased during these periods. According to the decrease in the glacier area and surface lowering rate, the mass wastage from the changes in the glacier surface elevation continuously decreased by 30%, from 0.0099 ± 0.0011 km^3 during 1988–1989 to 0.0070 ± 0.0011 km^3 during 2017–2018. As the glacial lake expanded continuously, the ratio of the mass contribution from lowering of the glacier

https://doi.org/10.5194/tc-2019-259
Preprint. Discussion started: 13 January 2020

surface to the lake volume has decreased significantly, from 41% during 1988–1989 to 9% during 2017–2018, and it exhibits a decreasing trend with a greater slope before 2000 than in the last decade.

Mass contributions from ice flow from the glacier terminal were approximately 10% of those due to lowering of the surface elevation, followed by an obvious fluctuation with an average mass budget of 0.0008 ± 0.0002 km^3 during the investigation period. In particular, during 1994–1995, 1996–1997, and 2003–2004, the fastest ice flow resulted in the most mass wastage (more than 0.0015 km^3). Overall, a slight decrease occurred in the mass contributions from ice flow during the last 30 years. The ratios of the ice flow contribution to lake volume were less than 5% during 1989–2018, which was accompanied by a slight decrease with significant fluctuations. In addition, the ratios during the last decade were less than 1%, except during 2009–2010 and 2010–2012. These results suggest that ice flow from the glacier terminal played a slight role in increasing the water volume of the proglacial lake.

Responding to huge fluctuations in areal changes in Longbasaba Glacier during the investigation period, the mass budgets resulting from the retreat of the glacier front varied significantly, with an average mass contribution of 0.0021 ± 0.0003 km^3, ranging from 0.0076 ± 0.0005 km^3 during 1993–1994 to nearly zero during 1989–1990 and 2004–2005. The terminal retreats according to the pattern of *category 1,* contributing a significantly greater mass budget to the lake volume than the other patterns, with mass contributions of > 0.0065 km^3 and ratios of >10% to the lake volume. In addition, the mass contributions from the retreat of the glacier front as described in *categories 2* and *3* were indistinguishable.

Overall, glacier shrinkage released an average mass of 0.0111 ± 0.0016 km^3 into the glacial lake with a slightly decreasing trend. The most mass contributions occurred during 1993–1994, 2000–2001, and 2003–2004, when the glacier terminal retreated as described in *category 1*; while glacier shrinkage as described in *category 2* contributed a larger mass budget relative to *Category 3*. During the last decade, the ratios of glacier change to lake volume were less than 16% with a mass wastage of less than 0.010 km^3. These results indicate that ice avalanches from the glacier terminal were an important source for lake expansion and were the predominant factor in the rapid mass wastage of the lake-terminated glacier.

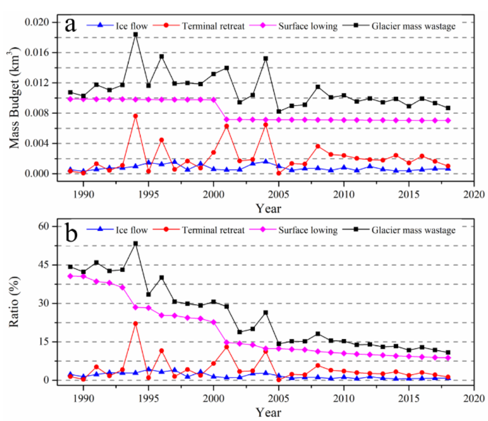

https://doi.org/10.5194/tc-2019-259
Preprint. Discussion started: 13 January 2020

Figure 9. Mass contributions **(a)** and ratios **(b)** of different patterns of glacier shrinkage to glacial lake water volume during 1989–2018. The black lines show the total mass contributions and ratios of glacier shrinkage to lake water volume.

5 Discussion

5.1 Uncertainty in the estimated mass contributions of glacier shrinkage to lake water volume

The variations in lake water volume were estimated based on the assumption that the proglacial lake experienced a negligible interannual change in water level during the investigation period. This ideal assumption is consistent with that made in previous studies. From 2003 to 2009, an insignificant average increase rate of 0.21 m a^{-1} was found in lake levels over the Third Pole based on ICESat altimetry data (Zhang et al., 2011; Zhang et al., 2017). The glacial lakes in the Himalayas exhibited no statistical variations in water level during the last decade based on the ICESat and CryoSat-2 data, although debris-contacted proglacial lakes have a slightly higher average increase rate of 0.8 m a^{-1} (Song et al., 2017). For proglacial lakes with the stable moraine dam and outlet, their small fluctuations in water level are ascribed to natural outflow regulations (Song et al., 2017). Based on several *in-situ* measurements, the water level of Longbasaba Lake showed an insignificant fluctuation (Yao et al., 2012; Wang et al; 2018). According to the mean lake depth of ~50 m, a mean change of 0.8 m a^{-1} in lake water level could contribute errors of ~1.5% relative to the estimated water volume in this study.

Mass wastage from lake-contacted glacier is composed of three components: evaporation/sublimation into the air, infiltration into the ground, and ice melt/avalanche into the proglacial lake. Mass budgets determined without considering the first two components would overestimate the mass contributions of the glacier changes to the lake water volume. Nevertheless, for glaciers developed in high mountain regions, the groundwater system and evaporation/sublimation in the glacier zone has a negligible impact on glacier hydrology and water resources relative to ice melt and avalanches (Kang et al., 1999; Brock et al., 2010; Liu et al., 2010; Zhang et al., 2012). Consequently, the methods used in this study, that is, ignoring evaporation/sublimation and infiltration, are reasonable and can be used to precisely reconstruct the mass contribution series of glacier degeneration to proglacial lake water volume.

Without considering the impacts of hypsometry and local topography, a mean lowering rate of -3.9 m a^{-1} was found for the glacier front elevation in the Himalayas (Song et al., 2017). In this study, we determined the glacier front elevation by combing the front position and the surface lowering rate and determined a precise series of elevations for the glacier front. Nevertheless, the mean surface lowering rate of the glacier tongue was used to indicate the elevation changes in the glacier front where the surface elevation commonly decreased with a higher ratio than in other locations. The assessed thicknesses of the glacier fronts were slightly overestimated in this study, which subsequently resulted in an overestimation of the mass contribution of the terminal motions.

https://doi.org/10.5194/tc-2019-259
Preprint. Discussion started: 13 January 2020

5.2 Mechanism of the variations in lake-terminated glacier shrinkage

The rapid mass wastage of glaciers causes rapid expansions of the glacier-contacted lakes (Fujita and Sakai, 2014; Immerzeel et al., 2014), which could expedite ice mass loss for parent glaciers (Gardelle et al., 2013; King et al., 2017). This is supported by the fact that proglacial lakes in the Himalayan range have experienced a rapid expansion extent of 36.5% during 2000–2014, which is more dramatic than that of other glacial lakes (Song et al., 2017). The lake-terminated glacier also showed an accelerating and greater mass melt than other glaciers, with mean glacier thickness changes of -0.65 ± 0.04 m a^{-1} during 1974–2000 and -0.80 ± 0.05 m a^{-1} during 1974–2000 in the Poiqu River Basin (Zhang et al., 2019). Nevertheless, Longbasaba Glacier has experienced an accelerating area decrease but accompanied by a decelerating and moderate glacier surface lowing.

Glaciers in the Himalayas are more sensitive to climate change than glaciers in other mountain ranges with higher annual temperatures, for example, Karakoram. In particular, a more significant response was found in the central Himalayas than in the western Himalayas and Karakoram (Fujita, 2008; Sakai et al., 2015). Most glaciers in the central Himalayas received their maximum accumulation in summer because of high monsoonal precipitation and high elevations (Ageta and Higuchi, 1984; Yao et al., 2012; Azam et al., 2018). Temperatures in the central Himalayas have increased significantly since 1960. A warming rate of 0.024 ± 0.004ºC a^{-1} was observed at Nyalam station during 1967–2017, followed by a decrease in precipitation of -0.76 ± 1.34 mm a^{-1} during 1960–2013 with a heterogeneous pattern (Zhang et al., 2019). Throughout the Himalayas, the observed glacier wastage is consistent with increasing temperature and decreasing precipitation (Azam et al., 2018). Along the Himalayan range glacier areal recession was more moderate than overall throughout High Mountain Asia over the last five to six decades, with a high variability in rates ranging from -0.07% a^{-1} to -1.38% a^{-1} and a mean retreat rate of -0.36% a^{-1} for 1960–2010 (Cogley, 2016; Azam et al., 2018). The average mass balance estimated using the geodetic method was less negative over the Himalayas than the global mean (Kääb et al., 2012; Gardelle et al., 2013), exhibiting a mass loss of -0.37 m w.e. a^{-1} between 1962–2015 (Azam et al., 2018). The central Himalayas have more gentle mass wastage than other regions in the Himalayas (Gardelle et al., 2013; King et al., 2017). In the Poiqu River Basin in the central Himalayas, glacier area has decreased by -0.52 ± 0.05% a^{-1} during 1964–2000 and increased to -0.72 ± 0.08% a^{-1} after 2000 (Zhang et al., 2019). For glacier surface elevation, an overall decrease of -0.38 ± 0.18 m a^{-1} occurred during 1974–2000, accompanying a more negative rate of -0.40 ± 0.14 m a^{-1} during 2000–2017 (Zhang et al., 2019). Nevertheless, compared to other lake-terminated glaciers in the central Himalayas, Longbasaba Glacier showed a specific response to climate change under the same pattern of climate change conditions, which suggests that other factors besides climate change play an important role in glacier recession.

Debris cover affects glacier mass budgets by controlling the heat conduction mechanism over the glacier surface, which depends on its thickness and the nature of the debris cover (Potter et al., 1998; Konrad et al., 1999; Brock et al., 2010; Reid and Brock, 2010; Lambrecht et al., 2011; Nicholson and Benn, 2013). However, several previous studies have determined that the surface-lowering rates of debris-free glaciers and debris-covered glaciers were accompanied by similar amounts of mass wastage in response to climate change (Kääb et al., 2012; Nuimura et al., 2012). In addition, the mass reduction

https://doi.org/10.5194/tc-2019-259
Preprint. Discussion started: 13 January 2020

of debris-covered glaciers is predominantly manifested as surface lowering without significant frontal retreat (Rowan et al., 2015; Banerjee, 2013). The internal ablation over the debris-covered tongue, for example, enlargement of englacial conduits, has a direct and/or indirect effect on the mass budgets through ice melt and collapse on the surface (Thompson et al., 2016; Benn et al., 2017). For lake-terminated glaciers with debris-covered tongues, fine-grained thick and intact debris cover insulates the ice from solar radiation, but this effect could be counteracted by significantly enhanced interaction between the glacier and lake in thermokarst features (Sakai et al., 2002; Buri et al., 2016; Miles et al., 2016; Watson et al., 2016). Under the same climate change conditions, Longbasaba Glacier showed a decreasing mass wastage during recent decades, which was followed by a contrary trend in the glacier tongue. Consequently, the debris cover of the Longbasaba Glacier played an important role in the rapid recession of the glacier tongue, but a further dynamic study is needed to assess the effect of the process.

Glacier surface velocities fluctuate with mass budgets at the decadal scale (Span and Kuhn, 2013; Dehecq et al., 2018). The ice flow of the glaciers in High Mountain Asia has commonly decreased, and a dramatic decreasing amplitude occurred in the Himalayas (Dehecq et al., 2018). In the Poiqu River Basin, the majority of lake-terminated glaciers exhibited faster ice flow than the other glaciers, which was followed by heterogeneous variations controlled by the topographic features of the glacier terminal (Zhang et al., 2019). This overall decrease in ice flow during a period of rapid glacier shrinkage suggests that mass loss commonly prompts glaciers to adjust their dynamics (Azam et al., 2012; Rowan et al., 2015; Bhattacharya et al., 2016). Recently, several glaciers in Karakoram have shown accelerating ice flow caused by positive mass budgets (Quincy et al., 2009; Azam et al., 2018). Unfortunately, the direct relationship between the changes in the surface velocity and the mass balance is not evident at the glacial or regional scales, which could be due to a lag in the response of ice flow to climate change (Heid and Kääb, 2012; Vincent and Moreau, 2016; Dechecq et al., 2018; Vincent and Moreau, 2016). In addition, the fluctuations in the velocity changes of Longbasaba Glacier displayed no obvious relationship with the changes in glacier area, length, and mass balances.

Longbasaba Glacier, which is a typical lake-terminated glacier with a debris-covered tongue, has experienced continuous and accelerating decrease in glacier area, but a decelerating mass wastage during the past three decades, which does not agree with the overall trends in the changes in ice mass for glaciers in the Himalayas and throughout the High Mountain Asia (Azam et al., 2018; Kääb et al., 2015; Bajracharya et al., 2015). In addition, the glacier tongue exhibited a contrary trend in mass loss relative to the glacier during the investigation period. For glaciers in direct contact with proglacial lakes, specific changes in area and ice mass are controlled by a complicated combination of processes and diverse local topographic conditions (Fujita and Sakai, 2014; Immerzeel et al., 2014; King et al., 2017; Song et al., 2017; Zhang et al., 2019). To assess the complex processes of the changes in the area and ice mass of lake-contacted glaciers, further detailed dynamic studies at the glacier-scale of the mass/energy interaction between glaciers and glacial lakes are urgently needed in the future.

https://doi.org/10.5194/tc-2019-259
Preprint. Discussion started: 13 January 2020

5.3 Potential triggers of GLOF for Longbasaba Lake

In the Himalayan range, GLOF events are predominantly triggered by the failure of moraine dams, caused by overtopping and/or self-destruction (Chen et al., 2006; Westoby et al., 2014; Rounce et al., 2017), which can potentially cause devastating disasters by transporting large amounts of debris (Allen et al., 2015). Large mass movements suddenly entering proglacial lakes, for example, ice/snow avalanches (Xu, 1987; Awal et al., 2010), rock falls and rockslides (Richardson and Reynolds, 2000), and extreme heavy precipitation (Harrison et al., 2018), can cause huge waves and the subsequent overtopping of bedrock or ice-core dams. The self-destruction of moraine dams is induced by piping/seepage, degradation of the ice-cores in the dams, dam collapse, and other triggers, for example, seismic events (Richardson and Reynolds, 2000; Chen et al., 2007; Westoby et al., 2014; Rounce et al., 2017; Harrison et al., 2018; Nie et al., 2018).

Current climate warming plays a predominant role in the degeneration of permafrost and ice cores in moraine dams, which can be a trigger for the failure of moraine dams (Vilímek et al., 2014; Harrison et al., 2018). In addition, extreme heat and extreme rainfall are potential triggers of GLOF events. Although no evident relationship was observed between climate change and an increase in GLOF events, it is predicted that the frequency of GLOF events increases during the next few decades by considering the lag times in the expansion and evolution of proglacial lakes (Harrison et al., 2018). Furthermore, under specific climate changes and their influence on hazards, complex glacier-proglacial lake interactions make glacier hazard study a challenging approach, but it is urgently needed (Marzeion et al., 2014; Shugar et al., 2017).

Ice avalanches with large masses from steep glacier fronts have been the predominant trigger of moraine dam failure in the Himalayan range (Awal et al., 2010; Nie et al., 2018) and have increased the potential for GLOFs (Sakai et al., 1998; Wang et al., 2008; Sakai et al., 2009; Gardelle et al., 2011). For Longbasaba Lake, numerous residual, various sized ice floes on the surface and bank of the lake were commonly observed by both *in-situ* measurements and remote detection during the investigation period and reflect the fact that ice avalanches commonly occurred (Yao et al., 2012; Wang et al., 2018). The glacier front retreat as described in *category 1*, for example, 1993–1994, 2000–20001, and 2003–2004, raised the lake water level by 6–11 m, assuming that the terminal motions released all of the mass of the ice avalanche at once and ignoring the influence of debris. While *category 2* retreat (e.g., 1999–2000, and 2001–2003) causes a water-level rise of more than 3 m. The recession as described in *category 3* can potentially raise the lake level by less than 2 m, especially after 2008. Ice avalanches create large amounts of ice and companying debris masses, which suddenly enter the proglacial lake and potentially create impact waves that trigger overtopping and failure of moraine dams. Although contributing much more masses than the glacier terminal motions, the glacier surface lowing released ice masses gradually and provided a slight increase in lake water level due to the stable outlet downstream of the lake basin. This suggests that ice avalanches potentially play a predominant role in the outburst risk of Longbasaba Lake. Piping/seepage in dams, rock-falls, and rockslides were observed infrequently (see Fig. 1c in Wang et al., 2018). However, these processes were considered to be negligible relative to ice avalanches from the glacier tongue.

Previous studies have revealed that the frequency and impact of GLOF events declined during the most recent decades in the Himalayan range (Harrison et al., 2018). This is partly ascribed to several successful measures carried out by local governments and communities to decrease the outburst possibility of glacial lakes, including stabilizing moraine dams and fluvial systems (Carrivick and Tweed, 2013). The moraine dams and outlet of Longbasaba Lake are monitored and maintained by local governments and scientists every year (Wang et al., 2018), including widening the river channel and stabilizing moraine dams and banks of the river channel before 2009. In 2010, during a small-scale ice avalanche, the moraine dams at the outlet of Longbasaba Lake were partly damaged, but did not fail. Eventually, the GLOF possibility of this proglacial lake has declined even during a time of rapid recession of the parent glacier, which may be manifested by the lagging response of Longbasaba Lake to climate change over a long-time scale (Harrison et al., 2018).

6 Conclusions

The evolution records for the shrinkage of Longbasaba Glacier and the expansion of the proglacial lake extend from 1988 to 2018, and the mass contributions from glacier shrinkage to the lake water volume were assessed and analyzed.

During the past three decades, Longbasaba Glacier has experienced a continuous and accelerating recession in the glacier area accompanied by the decelerating thinning and ice flow over the glacier surface. Consequently, the extent and water volume of Longbasaba Lake had expanded significantly at an accelerating rate. Lowering of the glacier surface played a predominant role in the mass contribution from glacier shrinkage to the lake water volume and was an order of magnitude higher than those from the motions of the glacier tongue. Overall, the mass contribution slightly decreased during the investigation period with dramatic fluctuations before 2008 due to a combination of a decelerating lowering rate of the glacier surface elevation and an accelerating decrease in the glacier area.

Longbasaba Glacier retreated with frequent ice avalanches, which suddenly released large amounts of ice into the proglacial lake and became the main potential trigger for failure of moraine dams and subsequent GLOF events. According to the areal expansion, decreasing mass contributions from the parent glacier shrinkage, and several improvements to the drainage system by local governments, the potential risk of GLOFs at Longbasaba Lake has continuously decreased during the last decade.

Code and data availability. The Landsat TM\ETM+\OLI images are available from the United States Geological Survey (USGS). The High Mountain Asia Gridded Glacier Thickness Changes from Multi-sensor DEMs, Version 1 is available from the National Snow and Ice Data Center (NSIDC) (Maurer et al., 2018). The free software module Co-registration of Optically Sensed Images and Correlation (COSI-Corr) is available from the Caltech Tectonics Observatory (TO) (Leprince et al., 2007). The Global Land Ice Velocity Extraction from Landsat 8 (GoLIVE), Version 1 is available from the NSIDC (Scambos et al., 2019). The *in-situ* echo sounder points with positions and water depths of Longbasaba Lake will be provided by Junfeng Wei upon request.

https://doi.org/10.5194/tc-2019-259
Preprint. Discussion started: 13 January 2020

Author contributions. JW and SL designed the study; JW, TZ, XW and YZ provided the formal analysis and validations. All authors discussed the results and contributed to the writing and editing of the manuscript.

Competing interests. The authors declare that they have no conflict of interest.

Acknowledgements. This work was founded by the fundamental programme of the National Natural Science Foundation of China (grant no. 41701061, 41761144075, and 41771075), the research project of Hunan University of Science and Technology (grant no. E51669), and the National Key Research and Development Program of China (grant no. 2018YFE0100100). We are grateful to the California Institute of Technology (CIT) for providing the not-for-profit institution with the COSI-Corr software.

References:

Ageta, Y. and Higuchi, K.: Estimation of Mass Balance Components of a Summer-Accumulation Type Glacier in the Nepal Himalaya, Geogr. Ann. Ser. Phys. Geogr., 66, 249-255, https://doi.org/10.2307/520698, 1984.

Allen, S. K., Rastner, P., Arora, M., Huggel, C. and Stoffel, M.: Lake outburst and debris flow disaster at Kedarnath, June 2013: hydrometeorological triggering and topographic predisposition, Landslides, 13(6), 1479-1491, https://doi.org/10.1007/s10346-015-0584-3, 2015.

Awal, R., Nakagawa, H., Fujita, M., Kawaike, K., Baba, Y. and Zhang, H.: Experimental study on Glacial Lake Outburst Floods due to wave overtopping and erosion of moraine dam, Ann. Disaster Prev. Res. Inst., Kyoto University 53(B), 583-594, 2010.

Ayoub, F., Leprince, S., and Avouac, J. P.: User's guide to COSI-CORR Co-registration of Optically Sensed Images and Correlation, Calif. Inst. Technol., https://doi.org/10.1109/IGARSS.2007.4423207, 2017.

Azam, M. F., Wagnon, P., Ramanathan, A., Vincent, C., Sharma, P., Arnaud, Y., Linda, A., Pottakkal, J. G., Chevallier, P., Singh, V. B., Berthier, E.: From balance to imbalance: a shift in the dynamic behaviour of Chhota Shigri glacier, western Himalaya, India. J. Glaciol., 58(208), 315-324, https://doi.org/10.3189/2012jog11j123, 2012.

Azam, M. F., Wagnon, P., Berthier, T., Vincent, C., Fujita, K. and Kargel, J. S.: Review of the status and mass changes of Himalayan Karakoram glaciers, J. Glaciol., 64(243), 61-74, https://doi.org/10.1017/jog.2017.86, 2018.

Bajracharya, S. R., Maharjan, S. B., Shrestha, F., Guo, W., Liu, S., Immerzeel, W. and Shrestha, B.: The glaciers of the Hindu Kush Himalayas: current status and observed changes from the 1980s to 2010, Int. J. Water Resour. D., 31(2), 161-173, https://doi.org/10.1080/07900627.2015.1005731, 2015.

Banerjee, A. and Shankar, R.: On the response of Himalayan glaciers to climate change, J. Glaciol., 59(215), 480-490, https://doi.org/10.3189/2013JoG12J130, 2013.

Benn, D. I., Sarah, T., Jason, G., Jordan, M., Adrian, L. and Lindsey, N.: Structure and evolution of the drainage system of a Himalayan debris-covered glacier, and its relationship with patterns of mass loss, The Cryosphere, 11, 2247-2264, https://doi.org/10.5194/tc-11-2247-2017, 2017.

Bhattacharya, A., Bolch, T., Mukherjee, K., Pieczonka, T., Kropáček, J. A. N. and Buchroithner, M. F.: Overall recession and mass budget of Gangotri Glacier, Garhwal Himalayas, from 1965 to 2015 using remote sensing data, J. Glaciol., 62(236), 1115-1133, https://doi.org/10.1017/jog.2016.96, 2016.

Bolch, T., Yao, T., Kang, S., Buchroithner, M. F., Scherer, D., Maussion, F., Huintjes, E. and Schneider, C.: A glacier inventory for the western Nyainqentanglha Range and the Nam Co Basin, Tibet, and glacier changes 1976-2009, The Cryosphere, 4, 419-433, https://doi.org/10.5194/tc-4-419-2010, 2010.

Bolch, T., Kulkarni, A. A., Kääb, A., Huggel, C., Paul, F., Cogley, J. G., Frey, H., Kargel, J. S., Fujita, K., Scheel, M., Bajracharya, S. and Stoffel, M.: The state and fate of Himalayan glaciers, Science, 336, 310-314, https://doi.org/10.1126/science.1215828, 2012.

Brock, B. W., Mihalcea, C., Kirkbride, M. P., Diolaiuti, G., Cutler, M. E. and Smiraglia, C.: Meteorology and surface energy fluxes in the 2005-2007 ablation seasons at the Miage debris-covered glacier, Mont Blanc Massif, Italian Alps, J. Geophys. Res., 115: D09106, https://doi.org/10.1029/2009JD013224, 2010.

Brun, F., Berthier, E., Wagnon, P., Kääb, A. and Treichler, D.: A spatially resolved estimate of High Mountain Asia glacier mass balances from 2000 to 2016, Nat. Geosci., 10(9), 668, https://doi.org/10.1038/NGEO2999, 2017.

Buri, P., Pellicciotti, F., Steiner, J. F., Miles, E. S. and Immerzeel, W. W.: A grid-based model of backwasting of supraglacial ice cliffs on debris-covered glaciers, Ann. Glaciol., 57(71), 199-211, https://doi.org/10.3189/2016aog71a059, 2016.

Carrivick, J. L. and Tweed, F. S.: Proglacial Lakes: character, behaviour and geological importance, Quat. Sci. Rev., 78, 34-52, https://doi.org/10.1016/j.quascirev.2013.07.028, 2013.

Chen, X., Cui, P., Yang, Z. and Qi, Y.: Debris Flows of Chongdui Gully in Nyalam County, 2002: Cause and Control, J. Glaciol. Geocryol., 28(5), 776-78, 1, 2006.

Chen, X., Cui, P., Yang, Z. and Qi, Y.: Risk assessment of glacial lake outburst in the Poiqu River basin of Tibet Autonomous region, J. Glaciol. Geocryol., 29(4), 509-516, https://doi.org/10.2514/1.26230, 2007.

Cogley, J. G.: Glacier shrinkage across High Mountain Asia, Ann. Glaciol., 57(71), 41-49, https://doi.org/10.3189/2016AoG71A040, 2016.

Copland, L., Sharp, M. J., Nienow, P. and Bingham, G.: The distribution of basal motion beneath a High Arctic polythermal glacier, J. Glaciol., 49(166), 407-414, https://doi.org/10.3189/172756503781830511, 2003.

Dehecq, A., Gourmelen, N., Gardner, A.S., Brun, F., Goldberg, D., Nienow, P., Berthier, E., Vincent, C., Wagnon, P. and Trouvé, E.: Twenty-first century glacier slowdown driven by mass loss in High Mountain Asia, Nat. Geosci., 12, 22-27, https://doi.org/10.1038/s41561-018-0271-9, 2018.

Emmer, A .: Glacier Retreat and Glacial Lake Outburst Floods (GLOFs). In Cutter, S. L. (Eds): Oxford research encyclopedia of natural hazard science. Oxford University Press, New York, 1-36, https://doi.org/10.1093/acrefore/9780199389407.013.27, 2017.

https://doi.org/10.5194/tc-2019-259
Preprint. Discussion started: 13 January 2020

Fahnestock, M., Scambos, T., Moon, T., Gardner, A., Haran, T. and Klinger, M.: Rapid large-area mapping of ice flow using Landsat 8, Remote Sens. Environ., 185. 84-94, https://doi.org/10.1016/j.rse.2015.11.023, 2015.

Fujita, K.: Effect of precipitation seasonality on climatic sensitivity of glacier mass balance, Earth Planet. Sci. Lett., 276(1), 14-19, https://doi.org/10.1016/j.epsl.2008.08.028, 2008.

Fujita, K., Suzuki, R., Nuimura, T. and Sakai, A.: Performance of ASTER and SRTM DEMs, and their potential for assessing glacial lakes in the Lunana region, Bhutan Himalaya, J. Glaciol., 54(185), 220-228, https://doi.org/10.3189/002214308784886162, 2008.

Fujita, K. and Sakai, A.: Modelling runoff from a Himalayan debris-covered glacier, Hydrol. Earth Syst. Sci., 18(7), 2679-2694, https://doi.org/10.5194/hess-18-2679-2014, 2014.

Gantayat, P., Kulkarni, A. V. and Srinivasan, J.: Estimation of ice thickness using surface velocities and slope: Case study at Gangotri Glacier, India. J. Glaciol., 60(220), 277-282, https://doi.org/ 10.3189/2014JoG13J078, 2014.

Gardelle, J., Arnaud, Y., and Berthier, E.: Contrasted evolution of glacial lakes along the Hindu Kush Himalaya mountain range between 1990 and 2009, Global Planet. Change, 75, 47-55, https://doi.org/10.1016/j.gloplacha.2010.10.003, 2011.

Gardelle, J., Berthier, E., Arnaud, Y. and Kääb, A.: Region-wide glacier mass balances over the Pamir - Karakoram - Himalaya during 1999-2011, The Cryosphere, 7, 1263-1286, https://doi.org/10.5194/tc-7-1263-2013, 2013.

Guo, W., Liu, S., Xu, L., Wu, L., Shangguan, D., Yao, X., Wei, J., Bao, W., Yu, P., Liu, Q. and Jiang, Z.: The second Chinese glacier inventory: data, methods, and results, J. Glaciol., 61(226), 1-16, https://doi.org/10.3189/2015JoG14J209, 2015.

Haritashya, U. K., Kargel, J. S., Shugar, D. H., Leonard, G. J., Strattman, K., Watson, C.S., and Regmi, D.: Evolution and Controls of Large Glacial Lakes in the Nepal Himalaya, Remote Sens., 10(5), 798, https://doi.org/10.3390/rs10050798, 2018.

Harper, J. T., Humphrey, N. F., Pfeffer, W. T., Huzurbazar, S. V., Bahr, D. B. and Welch, B. C.: Spatial variability in the flow of a valley glacier: Deformation of a large array of boreholes. J. Geophys. Res., 106, 8547-8562, https://doi.org/10.1029/2000JB900440, 2001.

Harrison, S., Kargel, J., Huggel, C., Reynolds, J., Shugar, D., Betts, R., Emmer, A., Glasser, N., Haritashya, U., Klimeš, J., Reinhardt, L., Schaub, Y., Wiltshire, A., Regmi, D. and Vilímek, V.: Climate change and the global pattern of moraine-dammed glacial lake outburst floods, The Cryosphere, 12, 1195-1209, https://doi.org/10.5194/tc-12-1195-2018, 2018.

Heid, T. and Kääb, A.: Repeat optical satellite images reveal widespread and long term decrease in land-terminating glacier speeds, The Cryosphere, 6, 467-478, https://doi.org/10.5194/tc-6-467-2012, 2012.

Huss, M.: Density assumptions for converting geodetic glacier volume change to mass change, The Cryosphere, 7, 877-887, https://doi.org/10.5194/tc-7-877-2013, 2013.

Immerzeel, W. W., Kraaijenbrink, P. D. A., Shea, J. M., Shrestha, A. B., Pellicciotti, F., Bierkens, M. F. P. and Jong, S. M. d.: High-resolution monitoring of Himalayan glacier dynamics using unmanned aerial vehicles, Remote Sens. Environ., 150, 93-103, https://doi.org/10.1016/j.rse.2014.04.025, 2014.

https://doi.org/10.5194/tc-2019-259
Preprint. Discussion started: 13 January 2020

The Cryosphere Discussions
Open Access
EGU

Kääb, A., Berthier, E., Nuth, C., Gardelle, J. and Arnaud, Y.: Contrasting patterns of early twenty-first-century glacier mass change in the Himalayas, Nature, 488, 495-498, https://doi.org/10.1038/nature11324, 2012.

Kääb, A., Treichler, D., Nuth, C. and Berthier, E.: Brief Communication: Contending estimates of 2003-2008 glacier mass balance over the Pamir-Karakoram-Himalaya, The Cryosphere, 9, 557-564, https://doi.org/10.5194/tc-9-557-2015, 2015.

Kang, E., Cheng, G., Lan, Y. and Jin, H.: A model for simulating the response of runoff from the mountainous watersheds of inland river basins in the arid area of northwest China to climatic changes, Sci. China Ser, 42(1), 52-63, https://doi.org/10.1007/BF02878853, 1999.

King, O., Quincey, D. J., Carrivick, J. L. and Rowan, A. V.: Spatial variability in mass loss of glaciers in the Everest region, central Himalayas, between 2000 and 2015, The Cryosphere, 11, 407-426, https://doi.org/ 10.5194/tc-11-407-2017, 2017.

Konrad, S. K., Humphrey, N. F. , Steig, E. J. , Clark, D. H. , Potter, N. and Pfeffer, W. T.: Rock glacier dynamics and paleoclimatic implications, Geology, 27(12), 1131-1134, https://doi.org/10.1130/0091-7613(1999)027<1131:RGDAPI>2.3.CO;2, 1999.

Krumwiede, B. S., Kamp, U., Leonard, G.J., Kargel, J. S., Dashtseren, A., Walther, M.: Recent glacier changes in the Mongolian Altai Mountains-Case studies from munkh khairkhan and tavan bogd, in: Global Land Ice Measurements from Space, Springer: Heidelberg, Germany, 481-508, 2014.

Lambrecht, A., Mayer, C., Hagg, W., Popovnin, V., Rezepkin, A., Lomidze, N. and Svanadze, D.: A comparison of glacier melt on debris-covered glaciers in the northern and southern Caucasus, The Cryosphere, 5, 525-538, https://doi.org/10.5282/ubm/epub.13559, 2011.

Leprince, S., Barbot, S., Ayoub, F. and Avouac, J. P.: Automatic and precise orthorectification, coregistration, and subpixel correlation of satellite images, application to ground deformation measurements, IEEE T. Geosci. Remote, 45(6), 1529-1558, https://doi.org/10.1109/tgrs.2006.888937, 2007.

Liu, Q., Liu, S., Zhang, Y., Wang, X., Zhang, Y., Guo, W. and Xu, J.: Recent shrinkage and hydrological response of Hailuogou glacier, a monsoon temperate glacier on the east slope of Mount Gongga, China. J. Glaciol, 56 (196), 215-224, https://doi.org/10.3189/002214310791968520, 2010.

Marzeion, B., Cogley, J. G., Richter, K. and Parkes, D.: Attribution of global glacier mass loss to anthropogenic and natural causes, Science, 345, 919-921, https://doi.org/10.1126/science.1254702, 2014.

Mathews, W. H.: Vertical Distribution of Velocity in Salmon Glacier, British Columbia, J. Glaciol, 3(26), 448-454, https://doi.org/10.3189/S0022143000017184, 1959.

Maurer, J., Rupper, S., and Schaefer., J.: High Mountain Asia Gridded Glacier Thickness Change from Multi-Sensor DEMs, Version 1. Boulder, Colorado USA. NASA National Snow and Ice Data Center Distributed Active Archive Center, https://doi.org/10.5067/GGGSQ06ZR0R8, 2018.

Miles, E. S., Pellicciotti, F., Willis, I. C., Steiner, J. F., Buri, P. and Arnold, N. S.: Refined energy-balance modelling of a supraglacial pond, Langtang Khola, Nepal, Ann. Glaciol., 57(71), 29-40, https://doi.org/10.3189/2016aog71a421, 2016.

https://doi.org/10.5194/tc-2019-259
Preprint. Discussion started: 13 January 2020

Nicholson, L., and Benn, D. I.: Properties of natural supraglacial debris in relation to modelling sub-debris ice ablation, Earth Surf. Processes Landforms, 38(5): 490-501, https://doi.org/10.1002/esp.3299, 2013.

Nie, Y., Sheng, Y., Liu, Q., Liu, L., Liu, S., Zhang, Y. and Song, C.: A regional-scale assessment of Himalayan glacial lake changes using satellite observations from 1990 to 2015, Remote Sens. Environ., 189, 1-13, https://doi.org/10.1016/j.rse.2016.11.008, 2017.

Nie, Y., Liu, Q., Wang, J., Zhang, Y., Sheng, Y. and Liu, S.: An inventory of historical glacial lake outburst floods in the Himalayas based on remote sensing observations and geomorphological analysis, Geomorphology, 308, 91-106, https://doi.org/10.1016/j.geomorph.2018.02.002, 2018.

Nuimura, T., Fujita, K., Yamaguchi, S. and Sharma, R. R.: Elevation changes of glaciers revealed by multitemporal digital elevation models calibrated by GPS survey in the Khumbu region, Nepal Himalaya, 1992-2008, J. Glaciol., 58(210), 648-656, https://doi.org/10.3189/2012JoG11J061, 2012.

Oerlemans, J.: Extracting a Climate Signal from 169 Glacier Records, Science, 308, 675-677, https://doi.org/10.1126/science.1107046, 2005.

Perutz, M. F.: Direct measurement of the velocity distribution in a vertical profile through a glacier, J. Glaciol., 1(5), 382-283, https://doi.org/10.3189/002214349793702593, 1949.

Potter, N., Steig, E. J., Clark, D. H., Speece, M. A., Clark, G. M. and Updike, A. B.: Galena Creek rock glacier revisited — new observations on an old controversy, Geogr. Ann.: Ser. A. Phys. Geo., 80(3-4), 251-265, https://doi.org/10.1111/j.0435-3676.1998.00041.x, 1998.

Quincey, D. J., Richardson, S. D., Luckman, A., Lucas, R. M., Reynolds, J. M., Hambrey, M. J. and Glasser, N. F.: Early recognition of glacial lake hazards in the Himalaya using remote sensing datasets, Global Planet. Change, 56, 137-152, https://doi.org/10.1016/j.gloplacha.2006.07.013, 2007.

Reid, T. D. and Brock, B. W.: An energy-balance model for debris-covered glaciers including heat conduction through the debris layer, J. Glaciol., 56: 903-916, https://doi.org/10.3189/002214310794457218, 2010.

Reynolds, J. M.: On the formation of supraglacial lakes on debris-covered glaciers, in: Nakawo, M., Raymond, C. F., and Fountain, A. (Eds.), Debris-Covered Glaciers, IAHS publications, 264, 153-161, 2000.

Richardson, S. D. and Reynolds, J. M.: An overview of glacial hazards in the Himalayas, Quat. Int., 65-66, 31-47, https://doi.org/10.1016/S1040-6182(99)00035-X, 2000.

Rounce, D., Watson, C. and McKinney, D.: Identification of Hazard and Risk for Glacial Lakes in the Nepal Himalaya using satellite imagery from 2000-2015, Remote Sens., 9(7), 654, https://doi.org/10.3390/rs9070654, 2017.

Rowan, A. V., Egholm, D. L., Quincey, D. J. and Glasser, N. F.: Modelling the feedbacks between mass balance, ice flow and debris transport to predict the response to climate change of debris-covered glaciers in the Himalaya, Earth Planet. Sci. Lett., 430, 427-438, https://doi.org/10.1016/j.epsl.2015.09.004, 2015.

Ruiz, L., Berthier, E., Masiokas, M., Pitte, P. and Villalba, R.: First surface velocity maps for glaciers of Monte Tronador, North Patagonian Andes, derived from sequential Pléiades satellite images, J. Glaciol., 61(229), 908-922, https://doi.org/10.3189/2015JoG14J134, 2015.

Sakai, A., Nakawo, M. and Fujita, K.: Melt rate of ice cliffs on the Lirung Glacier, Nepal Himalayas, 1996, Bull. Glacier Res. 16, 57-6, 6, 1998.

Sakai, A., Nakawo, M. and Fujita, K.: Distribution characteristics and energy balance of Ice cliffs on debris-covered glaciers, Nepal Himalaya, Arctic, Antarct. Alp. Res., 34, 12, https://doi.org/10.2307/1552503, 2002.

Sakai, A., Nishimura, K., Kadota, T. and Takeuchi, N.: Onset of calving at supraglacial lakes on debris-covered glaciers of the Nepal Himalaya, J. Glaciol. 55 (193), 909-917. 10.3189/002214309790152555, 2009.

Sakai, A., Nuimura, T., Fujita, K., Takenaka, S., Nagai, H. and Lamsal, D.: Climate regime of Asian glaciers revealed by GAMDAM glacier inventory, The Cryosphere, 9, 865-880, https://doi.org/10.5194/tc-9-865-2015, 2015.

Scambos, T., Fahnestock, M., Moon, T., Gardner, A., and Klinger, M.: Global Land Ice Velocity Extraction from Landsat 8 (GoLIVE), Version 1, Boulder, Colorado USA. NSIDC: National Snow and Ice Data Center, https://doi.org/10.7265/N5ZP442B, 2019.

Shugar, D. H., Clague, J. J., Best, J. L., Schoof, C., Willis, M. J., Copland, L., and Roe, G. H.: River piracy and drainage basin reorganization led by climate-driven glacier retreat, Nat. Geosci., 10, 370-375, https://doi.org/10.1038/ngeo2932, 2017.

Song, C., Sheng, Y., Wang, J., Ke, L., Madson, A. and Nie, Y.: Heterogeneous glacial lake changes and links of lake expansions to the rapid thinning of adjacent glacier termini in the Himalayas, Geomorphology, 280, 30-38, https://doi.org/10.1016/j.geomorph.2016.12.002, 2017.

Span, N. and Kuhn, M.: Simulating annual glacier flow with a linear reservoir model, J. Geophys. Res. 108, 4313, https://doi.org/10.1029/2002JD002828, 2003.

Thompson, S., Benn, D. I., Mertes, J. and Luckman, A.: Stagnation and mass loss on a Himalayan debris-covered glacier: processes, patterns and rates, J. Glaciol., 62(233), 467-485, https://doi.org/10.1017/jog.2016.37, 2016.

Veh, G., Korup, O., Roessner, S. and Walz, A.: Detecting Himalayan glacial lake outburst floods from Landsat time series, Remote Sens. Environ., 207, 84-97, https://doi.org/10.1016/j.rse.2017.12.025, 2018.

Vilímek, V., Emmer, A., Huggel, Ch., Schaub, Y. and Würmli, S.: Database of glacial lake outburst floods (GLOFs) - IPL Project No. 179, Landslides, 11, 161-165, https://doi.org/10.1007/s10346-013-0448-7, 2014.

Vincent, C. and Moreau, L.: Sliding velocity fluctuations and subglacial hydrology over the last two decades on Argentière glacier, Mont Blanc area, J. Glaciol. 62, 805-815, https://doi.org/10.1017/jog.2016.35, 2016.

Wang, X., Liu, S., Guo, W. and Xu, J.: Assessment and Simulation of Glacier Lake Outburst Floods for Longbasaba and Pida Lakes, China, Mt. Res. Dev., 28, 310-317, https://doi.org/10.1659/mrd.0894, 2008.

Wang, X., Liu, S., Guo, W., Yao, X., Jiang, Z., Han, Y.: Using Remote Sensing Data to Quantify Changes in Glacial Lakes in the Chinese Himalaya. Mt. Res. Dev., 32(2), 203-212, https://doi.org/ 10.1659/MRD-JOURNAL-D-11-00044.1, 2012.

https://doi.org/10.5194/tc-2019-259
Preprint. Discussion started: 13 January 2020

Wang, X., Liu, Q., Liu, S., Wei, J. and Jiang, Z.: Heterogeneity of glacial lake expansion and its contrasting signals with climate change in Tarim Basin, Central Asia, Environ. Earth Sci., 75, 696, https://doi.org/10.1007/s12665-016-5498-4, 2016.

Wang, X., Yang, C., Zhang, Y., Chai, K., Liu, S., Ding, Y., Wei, J., Zhang, Y., and Han, Y.: Monitoring and simulation of hydrothermal conditions indicating the deteriorating stability of a perennially frozen moraine dam in the Himalayas, J. Glaciol., 64(245), 407-416, doi: 10.1017/jog.2018.38, 2018.

Wang, S., Qin, D. and Xiao, C.: Moraine-dammed lake distribution and outburst flood risk in the Chinese Himalaya, J. Glaciol., 61(225), 115-126, https://doi.org/10.3189/2015JoG14J097, 2015.

Watson, C. S., Quincey, D. J., Carrivick. J. L. and Smith, M. W.: The dynamics of supraglacial ponds in the Everest region, central Himalaya, Global Planet. Change, 142, 14-27, https://doi.org/10.1016/j.gloplacha.2016.04.008, 2016.

Wei, J., Liu, S., Guo, W., Xu, J., Bao, W., and Shangguan, D.: Changes in glacier volume in the north bank of the Bangong Co Basin from 1968 to 2007 based on historical topographic maps, SRTM, and ASTER stereo images, Arct. Antarct. Alp. Res., 47(2), 155-165, http://dx.doi.org/10.1657/AAAR00C-13-129, 2015.

Westoby, M. J., Glasser, N. F., Hambrey, M. J., Brasington, J., Reynolds, J. M. and Hassan, M.: Reconstructing historic Glacial Lake Outburst Floods through numerical modelling and geomorphological assessment: Extreme events in the Himalaya, Earth Surf. Proc. Land., 39, 1675-1692, https://doi.org/10.1002/esp.3617, 2014.

Woodcock, C. E., Allen, R., Anderson, M., Belward, A., Bindschadler, R., Cohen, W., Gao, F., Goward, S. N., Helder, D., Helmer, E., Nemani, R., Oreopoulos, L., Schott, J., Thenkabail, P. S., Vermote, E. F., Vogelmann, J., Wulder, M. A., and Nemani, R.: Free access to Landsat imagery, Science, 320(5879), 1011, https://doi.org/10.1126/science.320.5879.1011a, 2008.

Wu, K., Liu, S., Jiang, Z., Xu, J., Wei, J. and Guo, W.: Recent glacier mass balance and area changes in the Kangri Karpo Mountains from DEMs and glacier inventories, The Cryosphere, 12, 103-121, https://doi.org/10.5194/tc-12-103-2018, 2018.

Xu, D.: Characteristics of debris flow caused by outburst of glacial lakes on the Boqu River in Xizang, China, J. Glaciol. Geocryol., 9(1), 23-34, https://doi.org/10.1007/BF00209443, 1987.

Yang, K., Lu, H., Yue, S., Zhang, G., Lei, Y., La, Z. and Wang, W.: Quantifying recent precipitation change and predicting lake expansion in the Inner Tibetan Plateau, Clim. Change, 147, 149-163, https://doi.org/ 10.1007/s10584-017-2127-5, 2018.

Yang, M., Wang, X., Pang, G., Wan, G. and Liu, Z.: The Tibetan Plateau cryosphere: Observations and model simulations for current status and recent changes, Earth-Sci. Rev., 190, 353-369, https://doi.org/10.1016/j.earscirev.2018.12.018, 2019.

Yao, X., Liu, S., Sun, M., Wei, J. and Guo, W.: Volume calculation and analysis of the changes in moraine-dammed lakes in the north Himalaya: a case study of Longbasaba lake, J. Glaciol., 58(210), 753-760, https://doi.org/10.3189/2012JoG11J048, 2012.

Zemp, M., Frey, H., Gärtner-Roer, I., Nussbaumer, S. U., Hoelzle, M., Paul, F., Haeberli, W., Denzinger, F., Ahlstrøm, A. P., Anderson, B., Bajracharya, S., Baroni, C., Braun, L. N., Cáceres, B. E., Casassa, G., Cobos, G., Dávila, L. R., Delgado Granados, H., Demuth, M. N., Espizua, L., Fischer, A., Fujita,

https://doi.org/10.5194/tc-2019-259
Preprint. Discussion started: 13 January 2020

The Cryosphere Discussions

K., Gadek, B., Ghazanfar, A., Hagen, J. O., Holmlund, P., Karimi, N., Li, Z., Pelto, M., Pitte, P., Popovnin, V. V., Portocarrero, C. A., Prinz, R., Sangewar, C. V., Severskiy, I., Sigurðsson, O., Soruco, A., Usubaliev, R., and Vincent, C.: Historically unprecedented global glacier decline in the early 21st century, J. Glaciol., 61, 745-762, doi:10.3189/2015JoG15J017, 2015.

Zhang, G., Xie, H., Kang, S., Yi, D. and Ackley, S. F.: Monitoring lake level changes on the Tibetan Plateau using ICESat altimetry data (2003-2009), Remote Sens. Environ., 115, 1733-1742, https://doi.org/10.1016/j.rse.2011.03.005, 2011.

Zhang, G., Yao, T., Xie, H., Wang, W. and Yang, W.: An inventory of glacial lakes in the Third Pole region and their changes in response to global warming, Global Planet. Change, 131, 148-157, https://doi.org/10.1016/j.gloplacha.2015.05.013, 2015.

Zhang, G., Yao, T., Shum, C. K., Yi, S., Yang, K., Xie, H., Feng, W., Bolch, T., Wang, L., Behrangi, A., Zhang, H., Wang, W., Xiang, Y. and Yu, J.: Lake volume and groundwater storage variations in Tibetan Plateau's endorheic basin, Geophys. Res. Lett., 44(11), 5550-5560, https://doi.org/10.1002/2017GL073773, 2017.

Zhang, G., Bolch, T., Allen, S., Linsbauer, A., Chen, W. and Wang, W.: Glacial lake evolution and glacier-lake interactions in the Poiqu River basin, central Himalaya, 1964-2017, J. Glaciol., 65(251), 347-365, https://doi.org/10.1017/jog.2019.13, 2019.

Zhang, Y., Hirabayashi, Y. and Liu, S.: Catchment-scale reconstruction of glacier mass balance using observations and global climate data: Case study of the Hailuogou catchment, south-eastern Tibetan Plateau, J. Hydrol., 444-445, 146-160, https://doi.org/10.1016/j.jhydrol.2012.04.014, 2012.